

Hindlimb Myology of the Monk Parakeet (Aves, Psittaciformes)

Julieta Carril,^{1,2*} María C. Mosto,^{2,3} Mariana B. J. Picasso,^{2,3} and Claudia P. Tambussi^{2,4}

¹Cátedra de Reproducción Animal, Instituto de Teriogenología, Facultad de Ciencias Veterinarias, Universidad Nacional de La Plata, Buenos Aires, Argentina

²Consejo Nacional de Investigaciones Científicas y Técnicas (CONICET), Argentina

³División Paleontología Vertebrados, Museo de La Plata, Universidad Nacional de La Plata, Buenos Aires, Argentina

⁴Centro de Investigaciones en Ciencias de la Tierra (CICTERRA-CONICET-UNC), Córdoba, Argentina

ABSTRACT We studied the hindlimb myology of the monk parakeet (*Myiopsitta monachus*). Like all parrots, it has zygodactyl feet enabling perching, climbing, hanging, moving easily among trees, and handling food. Muscles were described and weighed, and physiological cross-sectional area (PCSA) of four flexors and one extensor was calculated. In comparison to other muscles, the *M. tibialis cranialis* and the *M. fibularis brevis* show increased development and high PCSA values, and therefore, large potential force production. Also, a large proportion of muscle mass was involved in flexing the digits. We hypothesize that these muscle traits are associated with the arboreal locomotion and food manipulation habits. In the monk parakeet, the *M. extensor digitorum longus* sends a branch to the hallux, and the connection between the *M. flexor digitorum longus* and the *M. flexor hallucis longus* is type I (Gadow's classification). We reaffirm the presence of the *M. ambiens* as a plesiomorphic condition that disappears in most members of the order. Among Psittaciformes, the *M. fibularis brevis* is stronger and the *M. fibularis* weaker in arboreal species than in basal terrestrial ones (e.g., *Strigops*). *J. Morphol.* 275:732–744, 2014. © 2014 Wiley Periodicals, Inc.

KEY WORDS: *myiopsitta monachus*; zygodactyl feet; neotropical parrots; muscle; arboreal locomotion

INTRODUCTION

The monk parakeet *Myiopsitta monachus* (Boddaert, 1783) is one of the 148 species of Psittacinae (true parrots, parakeets, and macaws within the Psittacidae family) and constitutes one of the three (Tavares et al., 2006) or five (Wright et al., 2008) subclades within the Neotropical Tribe Arini. It is widely distributed in South America with a native range extending from southern Bolivia and southern Brazil to central Argentina. It is 29-cm long, with a wingspan of 48 cm, and it weighs 120 g. The monk parakeet is the only parrot that builds a stick nest rather than using a hole in a tree, which is typical for most Psittaciformes. This gregarious species often breeds by building communal nests with separate entrances for each couple (Collar, 1997 and bibliography cited

therein). Like all Psittaciformes, it has zygodactyl feet (toes II and III forward-oriented and toes I and IV backward-oriented) and a distinctive curved bill with a mobile upper mandible. This arrangement of the toes gives the birds the ability to perch (Bock and DeWitt Miller, 1959), climb, hang and easily move in trees and on the ground (Collar, 1997). Additionally, psittacids have a high manipulative ability, using their hindlimbs for feeding by holding small food items with one foot while the birds support themselves with the other one (Collar, 1997).

The Psittaciformes are one of the most speciose groups of nonpasseriform birds (Mayr, 2010). Although, they have been studied from multiple perspectives, current psittaciform taxonomy requires revision (Wright et al., 2008). Comparative gross myological information may serve as a basis for phylogenetics and systematics at various taxonomic levels (Vanden Berge, 1970; Raikow, 1987, 1994; McKittrick, 1991) as well as for studying the functional morphology of locomotion (Bock, 1994; Liem et al., 2001). Several studies have been performed in avian hindlimb myology (e.g., Hudson, 1937; Berger, 1960; Owre, 1967; Berman and Raikow, 1982; Raikow, 1985; Smith et al., 2006; Picasso et al., 2012; Zhang et al., 2012; Mosto et al., 2013). However, regarding psittaciforms, contributions are restricted to a few older studies where some general considerations were made in a comparative context with other birds (Giebel, 1862; Garrod, 1873, 1874a, b, 1876; Beddard,

*Correspondence to: Julieta Carril; Cátedra de Reproducción Animal, Instituto de Teriogenología, Facultad de Ciencias Veterinarias, Universidad Nacional de La Plata, Calle 60 y 118 S/N (1900), La Plata, Buenos Aires, Argentina. E-mail: julyetacarril@gmail.com

Received 22 July 2013; Revised 25 November 2013; Accepted 1 January 2014.

Published online 6 February 2014 in Wiley Online Library (wileyonlinelibrary.com). DOI 10.1002/jmor.20253

1898; Beddard and Parsons, 1893; Mitchell, 1913). The only extensive available description of a psittacid is that of Berman (1984) on the white-fronted amazon *Amazona albifrons* and the contribution (in Russian) by Zinoviev (2010) about *Micropsitta*. Besides myological descriptions of the Psittaciformes hindlimbs, few functional inferences about their locomotor habits have been made and there is no available muscular mass or physiological cross-sectional area data (PCSA).

As a consequence of the lack of knowledge in this field, the main objective of the present study is to analyze the pelvic limb myology of the monk parakeet as a basis for studies on its arboreal mode of life. We expect that, given the arboreal locomotion and their ability to handle food, the muscles responsible for flexion and rotation of the distal joints and digits (e.g., *M. tibialis cranialis*, *M. fibularis brevis*, and toe flexors) will have a greater development (enlarged origin sites, relatively high mass and/or higher muscle PCSA) in comparison to other hindlimb muscles.

MATERIALS AND METHODS

Eight adult specimens of *Myiopsitta monachus* (Boddaert, 1783) from Buenos Aires (La Plata) and Córdoba (Dean Funes) provinces (Argentina) were sacrificed by cervical dislocation, fixed by immersion in a 4% formaldehyde solution for 48 h and preserved in a 70% alcohol. Unilateral hindlimb dissections of all individuals were performed under a stereomicroscope at the Division Paleontología Vertebrados (Museo de La Plata, Argentina) from April 2012 to December 2012. The morphology of small muscles and tendons was studied using an iodine staining technique (Bock and Shear, 1972) to enhance visibility. The muscles were identified and carefully removed from their origin and insertion sites. Also, the attachment sites were represented on a drawing of the bones and photos were taken with a Nikon D-40 digital camera. Muscle descriptions follow the order of appearance from cranial to caudal and from superficial to deep muscles. The anatomical nomenclature follows Baumel et al. (1993).

Each muscle was weighed with a digital scale (0.001 g precision) and we calculated the percentage of individual muscle masses compared to total hindlimb mass and body mass. We assume that the left and right hindlimbs are symmetrical, and the latter percentage was calculated considering the sum of the measured muscles multiplied by two. The total mass of main flexors and extensors muscles on each articulation was calculated. Also, in attempt to understand the muscle force-generating capacity, the PCSA was calculated for the main muscles involved in arboreal locomotion and handling ability (i.e., the muscles responsible for flexion and rotation of the distal joints and digits; Berman and Raikow, 1982; Raikow, 1985; Moreno, 1990; Zinoviev, 2000; Volkov, 2004). These are the *mm. tibialis cranialis*, *fibularis brevis*, *fibularis longus*, *flexor digitorum longus*, and *flexor hallucis longus*. Because it is difficult to preserve the integrity of individual muscles during the process of muscle description, PCSA could be calculated only in four of the specimens dissected. The PCSA was estimated as muscle mass multiplied by the cosine of the average angle of pinnation, divided by the density of muscle tissue (1060 Kg/m³, Pennycuik, 1996) multiplied by the average fascicle length (Sustaita, 2008). Fascicle angles were measured relative to the axis of the muscle central tendon. Muscles were immersed in 15% HNO₃ for 24 h to dissolve the connective tissue that binds the fascicles and measure their length. The average angle of pinnation angle and the average fascicle length were obtained from 20 to

30 fibers of each muscle. Measurements were obtained from photographs using CorelDRAWX5 program.

Finally, to facilitate interpretation of morphological traits in a phylogenetic context, the observed traits were plotted onto a cladogram of psittaciform relationships. The tree used is based on the molecular phylogenetic analyses of Wright et al. (2008).

RESULTS

Descriptions of the Hindlimb Muscles

***M. iliotibialis cranialis (IC)*.** This is the most superficial muscle in the cranial aspect (Fig. 1a,b), and its proximal part covers the *mm. iliotrochanterici* (Fig. 2a,b). It is strap-like with a preacetabular origin (Fig. 5a), and it is fleshy along the cranial half of the *crista iliaca dorsalis*. The insertion is fleshy on the *ligamentum patellae* and the *crista cnemialis cranialis* (Fig. 6b).

***M. iliotibialis lateralis (IL)*.** It is mainly aponeurotic, and the fleshy portion is restricted to the middle region of the single belly. It presents the preacetabular portion and lacks the postacetabular one (Fig. 1a). It has an aponeurotic origin on the caudal half of the *crista iliaca dorsalis* (Fig. 5a). The distal aponeurotic portion is closely related to *M. femorotibialis lateralis et intermedius* and inserts on the *ligamentum patellae*.

***M. iliofibularis (IF)*.** It is a large muscle with a single belly and a triangular shape in the lateral view (Fig. 1a). It has a postacetabular origin, is aponeurotic at its cranial end, and is fleshy along the *crista dorsolateralis ilii* (Fig. 5a). The insertion is by a tendon that goes through the *ansa M. iliofibularis* onto the *tuberculum M. iliofibularis* of the lateral surface of the *fibula* (Fig. 6c).

***M. flexor cruris lateralis (FCL)*.** This muscle has two strap-like parts, *pars pelvica* (FCLp) and *pars accesoria* (FCLa; Figs. 1a,b, and 2b), clearly distinguishable by the fiber arrangement. The *pars pelvica* has a fleshy postacetabular origin on the dorso-caudal edge of the *ala ischii* (Fig. 5a) and inserts by a tendon on the proximal part of the medial surface of the *tibiotarsus* (Fig. 6d). In its distal portion, it fuses with the *M. flexor cruris medialis* and sends a tendon toward the aponeurotic joint of the *M. gastrocnemius*. The *pars accesoria* arises from the *pars pelvica* at its distal half and inserts on the distal part of the caudal surface of the *femur* (Fig. 5c), medially to the *fossa poplitea*.

***M. flexor cruris medialis (FCM)*.** It is a fleshy and strap-like muscle. It is the most superficial muscle on the caudal aspect of the hindlimb (Fig. 1a,b). It has a fleshy postacetabular origin on the caudal half of the ventral edge of the *ala ischii*, above the *fenestra ischiopubica* (Fig. 5a). The tendon of insertion goes between the *pars medialis* and *intermedia* of the *M. gastrocnemius* and inserts on the proximal part of the medial surface of the *tibiotarsus* (Fig. 6d).

***M. iliotrochantericus caudalis (ITC)*.** It is a large fleshy muscle with fleshy preacetabular

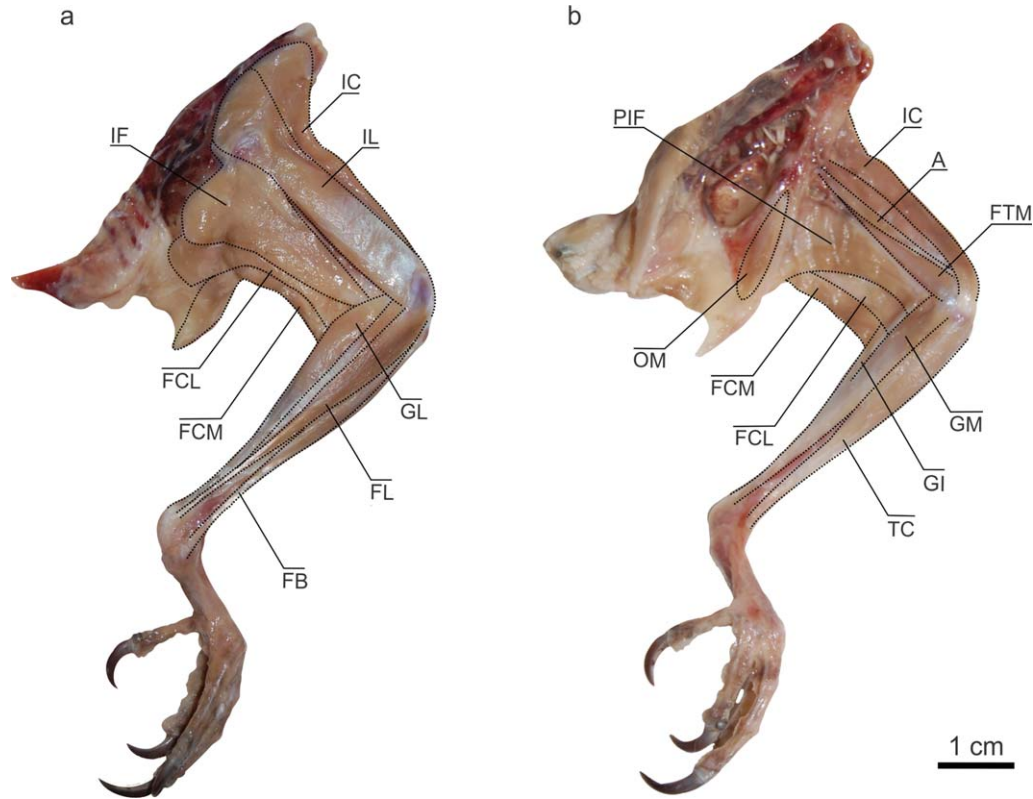


Fig. 1. *Myiopsitta monachus*, hindlimb muscles. Lateral (a) and medial (b) view of superficial muscles. Abbreviations: A, *M. ambiens*; FB, *M. fibularis brevis*; FCL, *M. flexor cruris lateralis*; FCM, *M. flexor cruris medialis*; FL, *M. fibularis longus*; FTM, *M. femoro-tibialis medialis*; IC, *M. iliotibialis cranialis*; IF, *M. iliofibularis*; IL, *M. iliotibialis lateralis*; GI, *M. gastrocnemius pars intermedia*; GL, *M. gastrocnemius pars lateralis*; GM, *M. gastrocnemius pars medialis*; OM, *M. obturatorius medialis*; PIF, *M. pubo-ischio-femoralis*; TC, *M. tibialis cranialis*.

origin on the cranial three-quarters of the *fossa iliaca dorsalis* (Figs. 2a and 5b). It inserts by a tendon on the proximo-lateral end of the *femur*, on one of the *impressiones iliotrochantericae*, between the insertions of the *m. iliofemoralis externus* and the *M. iliotrochantericus medius* (Fig. 5e).

M. iliotrochantericus cranialis (ITCr). This has a fleshy preacetabular origin on the cranial half of the inferior edge of the *fossa iliaca dorsalis* (Figs. 2b and 5b) and a tendinous insertion on the proximo-lateral end of the *femur*, specifically on the most distal of the *impressiones iliotrochantericae* (Fig. 5e).

M. iliotrochantericus medius (ITM). It has a fleshy preacetabular origin on the caudal part of the inferior edge of the *fossa iliaca dorsalis* (Figs. 2b and 5b). It inserts by a tendon on one of the *impressiones iliotrochantericae*, between the insertions of the *M. iliotrochantericus caudalis* and the *M. iliotrochantericus cranialis*, on the proximo-lateral end of the *femur* (Fig. 5e).

M. iliofemoralis externus (IFE). This is a small muscle with fleshy acetabular origin on the caudal end of the *crista iliaca dorsalis* (Figs. 2a and 5b) and with a small tendon of insertion on

the *trochanter femoris* (Fig. 5e), caudo-proximal to the insertion of the *M. iliotrochantericus caudalis*.

M. iliofemoralis internus (IFI). It is a small muscle with fleshy preacetabular origin on the caudo-ventral edge of the *ala preacetabularis* (Fig. 5b). It has a fleshy insertion on the caudal surface of the proximal third of the *femur* (Fig. 5c), between the level of insertions of the *M. ischiofemoralis* and *M. caudofemoralis*.

M. ischiofemoralis (ISF). It has a fleshy postacetabular origin on the *ala ischii* (Figs. 2c and 5b) and an insertion by a tendon on the middle region of the proximal part of the caudal surface of the *femur* (Fig. 5c), distal to the *impressiones obturatoriae*.

M. pubo-ischio-femoralis (PIF). This is a large strap-like muscle with two distinguishable bellies (*pars lateralis* and *medialis*; Figs. 1b and 2c). It has a fleshy postacetabular origin on the cranial half of the inferior edge of the *ala ischii*, on the membrane that covers the *fenestra ischio-pubica*, and on the upper edge of the cranial half of the pubis (Fig. 5b). It has a fleshy and tendinous insertion on the distal part of the caudal surface of the *femur* (Fig. 5c), between the *fossa poplitea* and the *crista supracondylaris medialis*.

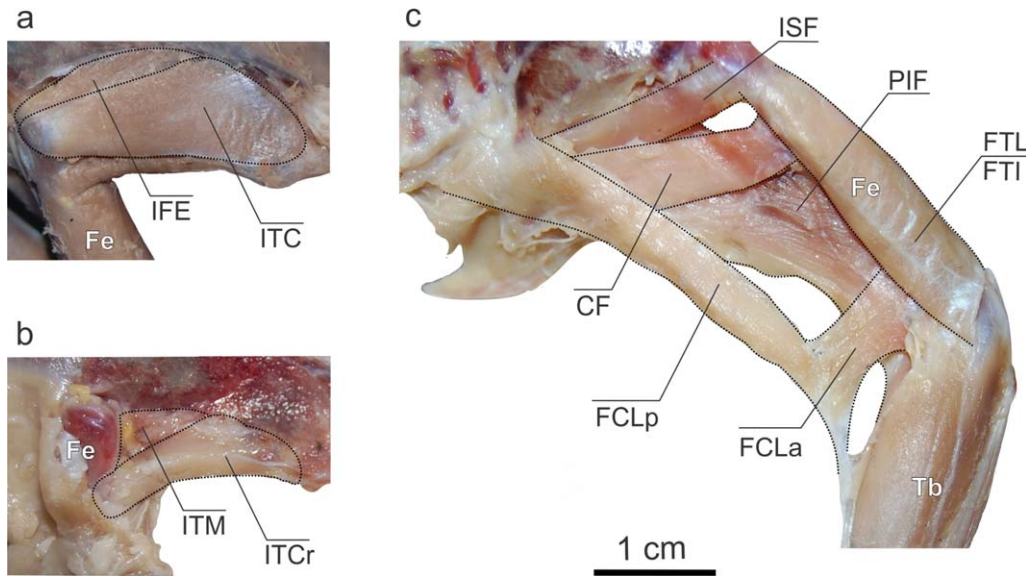


Fig. 2. *Myiopsitta monachus*, hindlimb muscles. Lateral view of deep muscles originated in the pelvis. Abbreviations: CF, *M. caudo-femoralis*; FCLa, *M. flexor cruris lateralis pars acesoria*; FCLp, *M. flexor cruris lateralis pars pelvica*; Fe, femur; FTI, *M. femorotibialis intermedius*; FTL, *M. femorotibialis lateralis*; IFE, *M. iliofemoralis externus*; ISF, *M. ischiofemoralis*; ITC, *M. ilirotrochantericus caudalis*; ITCr, *M. ilirotrochantericus cranialis*; ITM, *M. ilirotrochantericus medius*; PIF, *M. pubo-ischio-femoralis*; Tb, tibiotarsus.

***M. ambiens* (A).** This is a small muscle (Fig. 1b) with a preacetabular origin on the *tuberculum preacetabulare* of the *ilium* by a small tendon (Fig. 5b). Its belly occupies the medial side of the *femur* and the tendon of insertion crosses the *patella* and goes to the lateral region of the *tibiotarsus*. It inserts on the *M. flexor perforatus digiti II* at halfway along the fleshy portion of the latter muscle (Fig. 3d).

***M. obturatorius lateralis* (OL).** It is a small strap-like muscle with a fleshy postacetabular origin below the *foramen obturatum* (Fig. 5b). Only the *pars ventralis* is present. It inserts on the proximal region of the *femur* (Fig. 5c), below the insertion of the *M. obturatorius medialis*.

***M. obturatorius medialis* (OM).** It is a developed muscle with fleshy postacetabular origin on the medial surface of the *ala ischii* (Figs. 1b

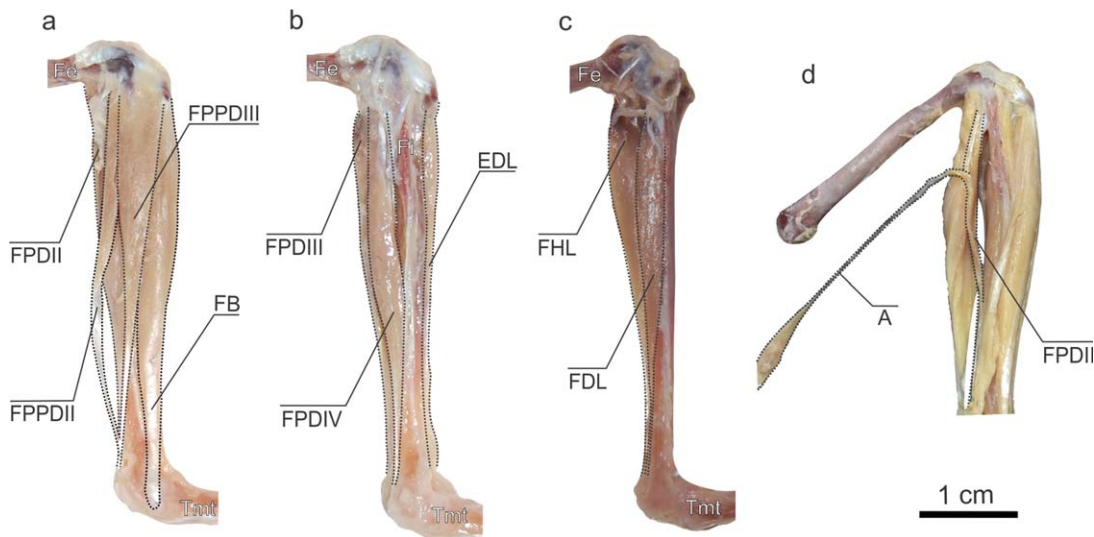


Fig. 3. *Myiopsitta monachus*, hindlimb muscles. Lateral (a–b) and medial (c) view of deep muscles originated in the femur and tibiotarsus. Detail of the insertion of the A on the FPDII (d). Abbreviations: A, *M. ambiens*; EDL, *M. extensor digitorum longus*; FB, *M. fibularis brevis*; FDL, *M. flexor digitorum longus*; Fe, femur; FHL, *M. flexor hallucis longus*; Fi, fibula; FPDII, *M. flexor perforatus digiti II*; FPDIII, *M. flexor perforatus digiti III*; FPDIV, *M. flexor perforatus digiti IV*; FPPDII, *M. flexor perforans et perforatus digiti II*; FPPDIII, *M. flexor perforans et perforatus digiti III*; Tmt, tarsometatarsus.

and 5a). Its belly goes through the *foramen obturatorum*. It has a fleshy and tendinous insertion on the proximo-caudal region of the *femur* on the most proximal of the *impressiones obturatoriae* (Fig. 5c).

M. caudofemoralis (CF). Only the *pars caudalis* is present. It has a tendinous origin on the *aponeurosis cruciata* of the *M. depressor caudae*, below the *pygostyle* (Fig. 2c). The insertion is fleshy and tendinous on the *linea intermuscularis caudalis*, at the proximal half of the caudal surface of the *femur* (Fig. 5c).

M. femorotibialis lateralis (FTL)* and *M. femorotibialis intermedius (FTI). These muscles are fused together (Fig. 2c) except in the proximal part of the origin where they are separated by the insertion of the *M. ilioprochantericus cranialis*. The origin is fleshy along the lateral surface and half of the cranial surface of the *femur* (Fig. 5d,e) whereas the insertion is aponeurotic on the *ligamentum patellae*.

M. femorotibialis medialis (FTM). It has a fleshy origin along the medial side of the femoral shaft (Figs. 1b and 5f) and a tendinous insertion on the proximal part of the *tibiotarsus*, below the *crista cnemialis cranialis* (Fig. 6b).

M. tibialis cranialis (TC). It is a large muscle, the most superficial of the cranial side of the *tibiotarsus* (Fig. 1b). The fleshy origin is placed between the *crista cnemialis cranialis* and *lateralis* (Fig. 6b) of the *tibiotarsus* on the proximal portion of the *M. extensor digitorum longus*, and it attaches by a tendon to the *fovea tendineus* of the *condylus lateralis* of the *femur* (Fig. 5d). Some fibers originate on the *ligamentum patellae*. The terminal strong tendon passes under the *retinaculum extensorium tibiotarsi* and inserts on the proximal middle third of the cranio-medial side of the *tarsometatarsus* (Fig. 6f).

M. fibularis longus (FL). It is a poorly developed muscle with aponeurotic origin between the *crista cnemialis cranialis* and the *lateralis* of the *tibiotarsus* (Figs. 1a and 6b), on the place of origin of the *M. tibialis cranialis*. It goes along the lateral surface of the *tibiotarsus* and inserts on the tibial cartilage by a single tendon. The cranial branch of the terminal tendon is absent.

M. fibularis brevis (FB). It is a well-developed muscle with double origin (Figs. 1a and 3a). The *caput fibulare* has a fleshy origin along the cranial surface of the *corpus fibulae* and the *caput tibiale* has a tendinous origin on the lateral surface of the proximal portion of the *tibiotarsus*, below the *crista cnemialis lateralis* (Fig. 6b,c). The proximal part is fleshy, and some of its fibers are laterally fused with some fibers of the *M. flexor perforans et perforatus digiti III* and medially fused with the *M. tibialis cranialis*, whereas the distal part is tendinous. The insertion of this mus-

cle is by a strong tendon on the cranio-lateral side of the *tarsometatarsus* (Fig. 6f).

M. gastrocnemius (G). It is the most superficial muscle of the caudal, medial, and lateral sides of the *tibiotarsus*, with three distinguishable portions (Fig. 1a,b). The *pars lateralis* (GL) has a fusiform shape and an origin by a short tendon on the *tuberculum M. gastrocnemialis lateralis* of the *femur* (Fig. 5e). The *pars intermedia* (GI) also has a fusiform shape and originates by a short tendon on the medial edge of the *fossa poplitea* (Fig. 5c). The *pars medialis* (GM) is strap-like with a fleshy and tendinous origin on the *condylus medialis* of the *femur* and on the *crista cnemialis lateralis* of the *tibiotarsus* (Figs. 5f and 6d). The three parts converge in a wide strong tendon that goes through the tibial cartilage and forms a tendinous sheath for terminal tendons of the digital flexors.

M. extensor digitorum longus (EDL). This muscle has two bellies and a fleshy origin between the *crista cnemialis cranialis* and the *lateralis* and along the proximal third of the cranio-medial side of the *tibiotarsus* (Figs. 3b and 6b). The tendon of insertion passes under the *pons supratendineus* and through the *tibiotarsus-tarsometatarsus* joint, bifurcates halfway along the *tarsometatarsus* and sends one branch to the hallux and three main branches to digits II, III, and IV (Fig. 4d). These tendons have smaller accessory tendons that insert on proximal phalanges of each digit, while the main tendons insert on the articular surface of the ungual phalanges (*tuberculum extensorium*) (Fig. 6f).

M. flexor digitorum longus (FDL). It is a large muscle with a fleshy origin on the proximal half of the *tibiotarsus* and on the *fibula* (Figs. 3c, 4a, and 6a), covering mainly the caudal sides and also part of their lateral and medial sides. The tendon of insertion goes through the *canal hypotarsi* (Fig. 6g) and, at the distal part of the *tarsometatarsus*, connects with the tendon of the *M. flexor hallucis longus* by the *vinculum tendinum flexorum*. Then it divides toward digits II, III, and IV. These three branches insert on the *tuberculum flexorium* of each ungual phalanx but also on the distal end of phalanx 3 of digit III and phalanx 4 of digit IV (Fig. 6e).

M. flexor hallucis longus (FHL). It has a fleshy and tendinous origin on the *fossa poplitea* of the *femur* (Figs. 3c, 4a, and 5c). The tendon of insertion passes through the *canal hypotarsi* (Fig. 6g), connects with the tendon of the *M. flexor digitorum longus* by the *vinculum tendinum flexorum* (Fig. 4b), and inserts on the proximal end of the ventral side of the ungual phalanx of digit I, on the *tuberculum flexorium* (Fig. 6e).

M. flexor perforans et perforatus digiti II (FPPDII). It is a muscle with a fleshy origin on the caudal side of the distal end of the *femur* (Figs. 3a and 5c) and with insertion by a tendon

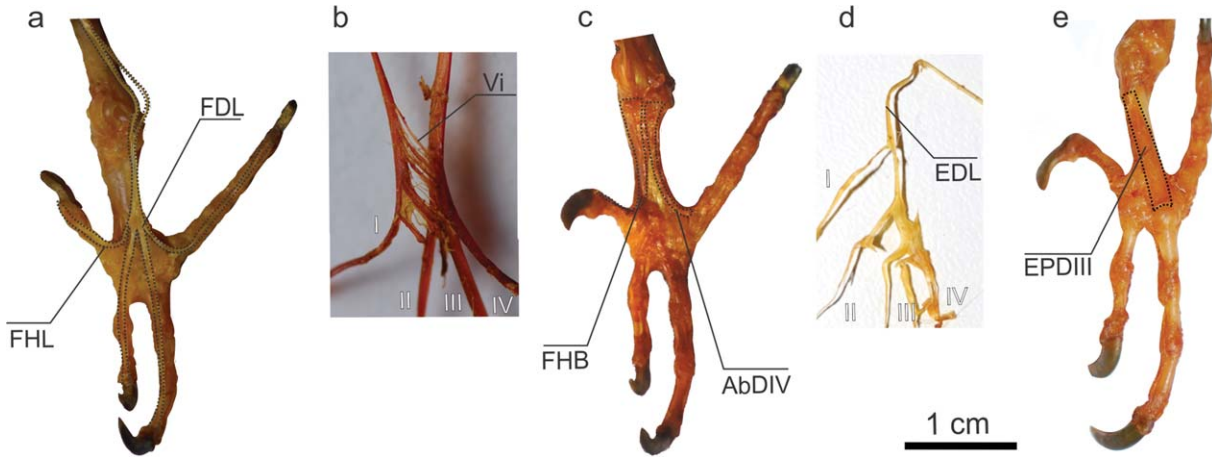


Fig. 4. *Myiopsitta monachus*, hindlimb muscles. Caudal (a, c) and cranial (e) view of the digit muscles. Details of the vinculum (Vi) between FDL and FHL (3X increase) (b) and the branch of the MEDL to the hallux (d). Abbreviations: I-IV, digits I to IV; AbDIV, *M. abductor digiti IV*; EDL, *M. extensor digitorum longus*; EPDIII, *M. extensor proprius digiti III*; FDL, *M. flexor digitorum longus*; FHB, *M. flexor hallucis brevis*; FHL, *M. flexor hallucis longus*.

perforated by the *M. flexor digitorum longus*. This tendon runs along digit II, bifurcates, and inserts on both sides of the proximal end of phalanx 2 (Fig. 6e).

M. flexor perforans et perforatus digiti III (FPPDIII). It is a muscle with a fleshy origin and with a small tendon origin on the *crista cnemialis lateralis* of the *tibiotarsus* (Figs. 3a and 6c). Its proximal half is fused to the *M. fibularis brevis*. The tendon of insertion is perforated by the *M. flexor digitorum longus* and is connected to the tendon of the *M. flexor perforatus digiti III* by a *vinculum tendinum flexorum*. Then it bifurcates and inserts at both sides of the proximal side of the phalanx 3 of digit III (Fig. 6e).

M. flexor perforatus digiti II (FPDII). It has a fleshy double origin on the caudal side of the proximal part of the fibula and on the *condylus lateralis* of the *femur* (Figs. 3a, 5c, and 6a). The tendon of insertion goes through the tibial cartilage and the *sulcus hypotarsi* (Fig. 6g) and inserts on the proximal part of the lateral side of phalanx 1 of digit II (Fig. 6e).

M. flexor perforatus digiti III (FPDIII). It has a tendinous origin on the caudal side of the distal end of the *femur*, between the *condylus lateralis* and *medialis* (Figs. 3b and 5c). The tendon is pierced by the tendons of the *M. flexor perforans et perforatus digiti III* and *M. flexor digitorum longus*, bifurcates, and inserts on the medial and lateral side of the phalanx 2 of the digit III (Fig. 6e).

M. flexor perforatus digiti IV (FPDIV). It has a fleshy and tendinous origin on the caudal side of the distal region of the *femur* (Figs. 3b and 5c), distal to the origin of the *M. flexor perforans et perforatus digiti II*. The tendon is pierced by the *M. flexor digitorum longus* and has three points of insertion on digit IV: on the middle of the medial

side of phalanx 1, on the distal end of the medial side of phalanx 2, and on the lateral side of the proximal region of phalanx 3 (Fig. 6e).

M. extensor proprius digiti III (EPDIII). It has a fleshy origin along the cranial side of the *tarsometatarsus* (Figs. 4e and 6f) and fleshy insertion on the dorsal side of the proximal portion of phalanx 1 of digit III (Fig. 6f).

M. abductor digiti II (AbDII). It has a fleshy origin on the *trochlea metatarsi I* on the cranial side of the *tarsometatarsus* (Fig. 6f) and a fleshy insertion on the dorsal side of the proximal end of phalanx 1 of digit II (Fig. 6f).

M. flexor hallucis brevis (FHB). This muscle is located underneath the tendon of the flexors of the digits. It has a fleshy origin on the proximal half of the caudo-medial side of the *tarsometatarsus* (Figs. 4c and 6e) and a tendinous insertion on the medial part of the ventral side of phalanx 1 of digit I (Fig. 6e).

M. abductor digiti IV (AbDIV). It has a fleshy origin on the proximal quarter of the caudo-lateral side of the *tarsometatarsus* (Figs. 4c and 6e) and a tendinous insertion on the medial side of the proximal end of phalanx 1 of digit IV (Fig. 6e).

Finally, of the hindlimb muscles that are generally present in Aves (Baumel et al., 1993), *mm. iliotibialis medialis*, *plantaris*, *popliteus*, *extensor hallucis longus*, *adductor digiti II*, *extensor brevis digiti III*, *extensor brevis digiti IV* and *lumbricales* were not found in the monk parakeet.

Hindlimb Muscle Masses and PCSA

The average body mass of the specimens was 117.97 g (SE: 3.5, $n = 8$) and the total muscle mass of both hindlimbs represents 6.535% of the body mass. The percentage of each individual muscle mass with respect to the total hindlimb mass

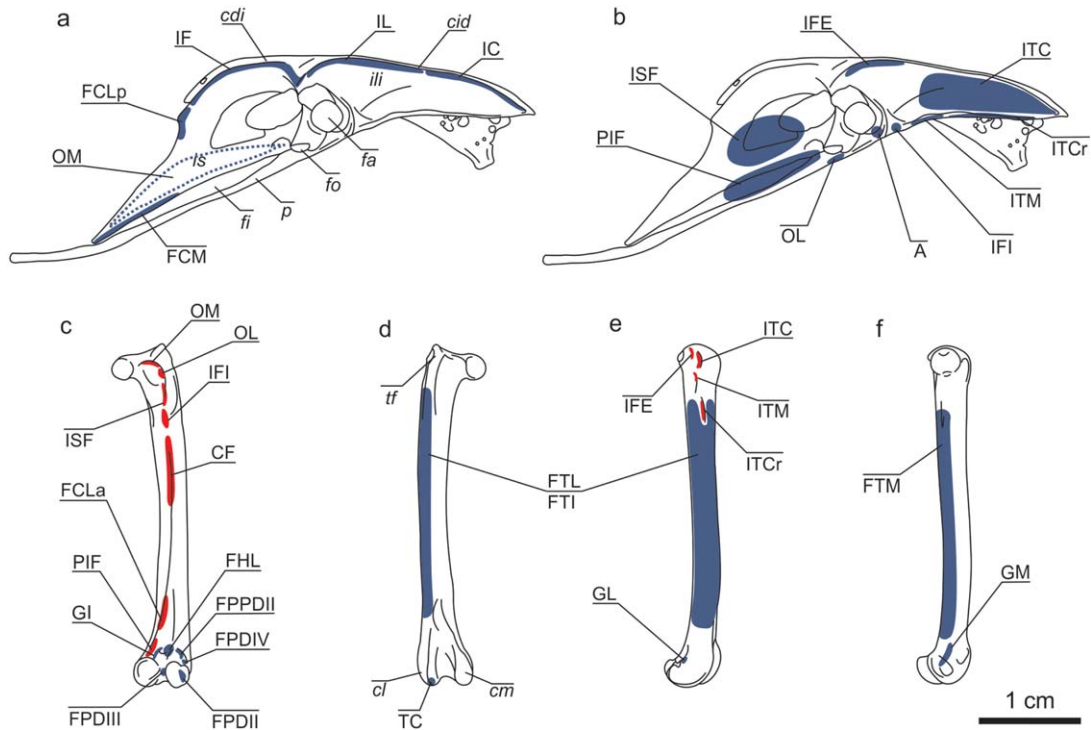


Fig. 5. *Myiopsitta monachus*, pelvis and femur. Sketches of the lateral view of the pelvis with the origins of the superficial (a) and deep (b) muscles drawn. The dotted line (the origin of the OM) is located in the medial aspect of the pelvis. Sketches of the femur (c–f) from left to right: caudal, cranial, lateral and medial view. Origins are indicated with blue and the insertions with red. Abbreviations: A, *M. ambiens*; cdi, *crista dorsolateralis ilii*; CF, *M. caudofemoralis*; cid, *crista iliaca dorsalis*; cl, *condylus lateralis*; cm, *condylus medialis*; FCLa, *M. flexor cruris lateralis pars accesoria*; FCLp, *M. flexor cruris lateralis pars pelvica*; FCM, *M. flexor cruris medialis*; FHL, *M. flexor hallucis longus*; fa, *foramen acetabuli*; fi, *fenestra ischiopubica*; fo, *foramen obturatum*; FPDII, *M. flexor perforatus digiti II*; FPDIII, *M. flexor perforatus digiti III*; FPDIV, *M. flexor perforatus digiti IV*; FPPDII, *M. flexor perforans et perforatus digiti II*; FTI, *M. femorotibialis intermedius*; FTL, *M. femorotibialis lateralis*; FTM, *M. femorotibialis medialis*; GI, *M. gastrocnemius pars intermedia*; GL, *M. gastrocnemius pars lateralis*; GM, *M. gastrocnemius pars medialis*; IC, *M. iliotibialis cranialis*; IF, *M. iliofibularis*; IFE, *M. iliofemorales externus*; IFI, *M. iliofemorales internus*; IL, *M. iliotibialis lateralis*; ili, *ilium*; is, *ischium*; ISF, *M. ischiofemorales*; ITC, *M. iliotrochantericus caudalis*; ITCr, *M. iliotrochantericus cranialis*; ITM, *M. iliotrochantericus medius*; OL, *M. obturatorius lateralis*; OM, *M. obturatorius medialis*; p, *pubis*; PIF, *M. pubo-ischio-femorales*; TC, *M. tibialis cranialis*; tf, *trochanter femoris*.

ranges from 0.104% (IFI and AbdII) to 11.032% (FTL + FTI; Table 1).

The main flexor muscles of the hip joint constituted a lower percentage of body mass compared to the extensors (0.813% vs. 0.910%). Flexors of the knee joint constituted 1.212% of body mass, compared to 0.721% for the extensors. For the ankle joint, the main flexor represented 0.325%, compared to the extensors' 0.523%. The toes flexors represent together 1.046% of the body mass, while the extensors represent 0.174% (Fig. 7).

PCSA values were calculated for five hindlimb muscles: TC ($11.298 \pm 0.36 \text{ mm}^2$), FDL ($10.179 \pm 0.68 \text{ mm}^2$), FB ($8.811 \pm 0.70 \text{ mm}^2$), FHL ($6.157 \pm 0.12 \text{ mm}^2$), and FL ($3.576 \pm 0.28 \text{ mm}^2$).

DISCUSSION

Phylogenetic Context for the Muscular Features

For a long time, the hindlimb muscular formula proposed by Gadow (1894) was considered sufficient to describe the appendicular myology of

birds. According to Berger (1956), its application in taxonomy becomes ineffective due to intraspecific muscle variation. Nevertheless, Zinoviev (2007) pointed out the importance of the formula in assessing of higher avian levels. Since the mid-twentieth century, many anatomists have been devoted to describing all the muscles of the pelvic limb, and knowledge of that subject has grown accordingly, but progress was practically negligible for the group Psittaciformes.

We found some differences between the muscles of the monk parakeet and descriptions for the white-fronted amazon (Berman, 1984; Fig. 8: trends F/f to N/n). For example, the *M. ambiens* and the *M. abductor digiti II* are present in the monk parakeet but absent in the white-fronted amazon. The *M. extensor brevis digiti IV*, the *M. extensor hallucis longus*, and the *M. lumbricales*, all absent in the monk parakeet, are poorly developed in the white-fronted amazon. The foot muscle *M. extensor propius digiti III accesorius* is absent in the monk parakeet but is very well developed in the white-fronted amazon, while the *M. extensor*

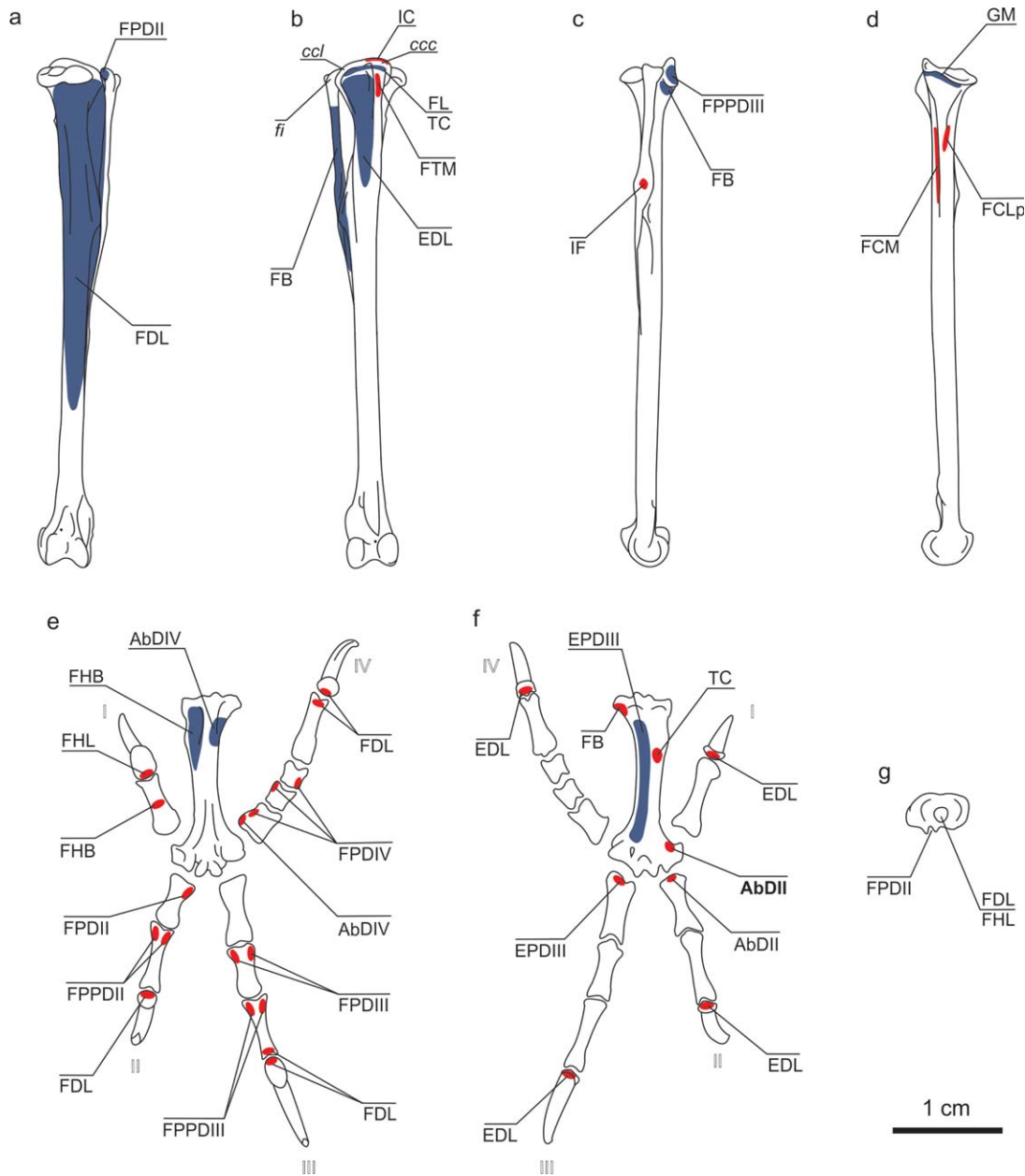


Fig. 6. *Myiopsitta monachus*, tibiotarsus, tarsometatarsus and digits. Sketches of the tibiotarsus (a–d) from left to right: caudal, cranial, lateral and medial view. Sketches of the tarsometatarsus and phalanges in caudal (e) and cranial (f) view. Sketch of the tarsometatarsus in proximal end view (g). Origins are indicated with blue and the insertions with red. Abbreviations: I–IV, digits I to IV; AbDII, *M. abductor digiti II*; AbDIV, *M. abductor digiti IV*; ccc, crista cnemialis cranialis; ccl, crista cnemialis lateralis; EDL, *M. extensor digitorum longus*; EPDIII, *M. extensor proprius digiti III*; FB, *M. fibularis brevis*; FCLp, *M. flexor cruris lateralis pars pelvica*; FCM, *M. flexor cruris medialis*; FHB, *M. flexor hallucis brevis*; FHL, *M. flexor hallucis longus*; fi, fibula; FDL, *M. flexor digitorum longus*; FL, *M. fibularis longus*; FPDII, *M. flexor perforatus digiti II*; FPDIII, *M. flexor perforatus digiti III*; FPDIV, *M. flexor perforatus digiti IV*; FPPDII, *M. flexor perforans et perforatus digiti II*; FPPDIII, *M. flexor perforans et perforatus digiti III*; FTM, *M. femorotibialis medialis*; GM, *M. gastrocnemius pars medialis*; IC, *M. iliotalialis cranialis*; IF, *M. iliofibularis*; TC, *M. tibialis cranialis*.

propius digiti III is present in both species (*M. extensor digitorum brevis medialis* and *M. extensor digitorum brevis lateralis*, respectively, sensu Zinoviev, 2003a). The white-fronted amazon shows two points of insertion of the *M. tibialis cranialis* (there is only one in the monk parakeet). The *M. iliofibularis* is formed by a single belly in the

monk parakeet (whereas there are two in the white-fronted amazon) and the *M. flexor perforatus digiti II* has the fibular and also the femoral origin in the monk parakeet (while the femoral origin is absent in the white-fronted amazon). The *M. flexor perforans et perforatus digiti II*, which is imperforated in the white-fronted amazon, is perforated

TABLE 1. Hindlimb muscles masses of *Myiopsitta monachus*

Muscle	Abb	Mass (g.)	SE	% hl	% bm	Main muscle action
<i>M iliobtibialis cranialis</i>	IC	0.197	0.010	5.097	0.333	<i>femur</i> flexion*
<i>M iliobtibialis lateralis</i>	IL	0.126	0.018	3.279	0.214	<i>femur</i> abduction
<i>M iliobfibularis</i>	IF	0.330	0.021	8.550	0.559	<i>tibiotarsus</i> flexion*
<i>M flexor cruris lateralis</i>	FCL	0.245	0.033	6.355	0.415	<i>tibiotarsus</i> flexion* and <i>femur</i> extension
<i>M flexor cruris medialis</i>	FCM	0.140	0.004	3.634	0.238	<i>tibiotarsus</i> flexion*
<i>M iliobtrochantericus caudalis</i>	ITC	0.195	0.009	5.048	0.330	<i>femur</i> flexion*
<i>M iliobtrochantericus cranialis</i>	ITCr	0.051	–	1.323	0.086	<i>femur</i> flexion* and inward rotation
<i>M iliobtrochantericus medius</i>	ITM	0.038	–	0.986	0.064	<i>femur</i> flexion* and inward rotation
<i>M iliobfemoralis externus</i>	IFE	0.021	0.001	0.550	0.036	<i>femur</i> abduction
<i>M iliobfemoralis internus</i>	IFI	0.004	–	0.104	0.007	<i>femur</i> adduction, flexion and outward rotation
<i>M ischiofemoralis</i>	ISF	0.082	0.005	2.117	0.138	<i>femur</i> extension*
<i>M pubo-ischio-femoralis</i>	PIF	0.302	0.010	7.842	0.513	<i>femur</i> extension*
<i>M ambiens</i>	A	0.015	0.003	0.394	0.026	aid the FPDII*
<i>M obturatorius lateralis</i>	OL	0.012	–	0.311	0.020	<i>femur</i> outward rotation
<i>M obturatorius medialis</i>	OM	0.063	0.011	1.624	0.106	<i>femur</i> outward rotation and abduction
<i>M caudofemoralis</i>	CF	0.153	0.008	3.964	0.259	<i>femur</i> extension*
<i>M femorotibialis lateralis</i> + <i>intermedius</i>	FTL + FTI	0.425	0.013	11.032	0.721	<i>tibiotarsus</i> extension*
<i>M femorotibialis medialis</i>	FTM	0.065	0.004	1.686	0.110	<i>tibiotarsus</i> inward rotation
<i>M tibialis cranialis</i>	TC	0.192	0.011	4.975	0.325	<i>tarsometatarsus</i> flexion*
<i>M fibularis longus</i>	FL	0.056	0.010	1.445	0.094	<i>tarsometatarsus</i> extension*
<i>M fibularis brevis</i>	FB	0.135	0.014	3.510	0.229	<i>tibiotarsus</i> inward rotation
<i>M gastrocnemius</i>	G	0.253	0.018	6.571	0.429	<i>tarsometatarsus</i> extension*
<i>M extensor digitorum longus</i>	EDL	0.103	0.011	2.659	0.174	digits extension*
<i>M flexor digitorum longus</i>	FDL	0.162	0.013	4.192	0.274	digits II-IV flexion*
<i>M flexor hallucis longus</i>	FHL	0.069	0.006	1.785	0.117	digits I flexion / aid the FDL*
<i>M flexor hallucis brevis</i>	FHB	0.017	0.003	0.446	0.029	digit I flexion
<i>M flexor perforans perforatus digiti II</i>	FPPDII	0.052	0.004	1.349	0.088	digit II flexion*
<i>M flexor perforans perforatus digiti III</i>	FPPDIII	0.100	0.004	2.594	0.170	digit III flexion*
<i>M flexor perforatus digiti II</i>	FPDII	0.028	0.002	0.737	0.048	digit II flexion*
<i>M flexor perforatus digiti III</i>	FPDIII	0.095	0.009	2.464	0.161	digit III flexion*
<i>M flexor perforatus digiti IV</i>	FPDIV	0.096	0.005	2.482	0.162	digit IV flexion*
<i>M extensor proprius digiti III</i>	EPDIII	0.020	–	0.519	0.034	digit III extension*
<i>M abductor digiti II</i>	AbDII	0.004	–	0.104	0.007	digit II extension*
<i>M abductor digiti IV</i>	AbDIV	0.010	0	0.259	0.017	digit IV adduction

Abb, abbreviations of each dissected muscle; Mass, muscle mean weight; SE, standard error (df: n-1); % hl: percentage of each muscle in relation to the hindlimb mass; % bm, percentage of each muscle in relation to the body mass; Main muscle action, according to Raikow (1985),

*indicates the muscles used in Figure 7.

by the tendon of insertion of the *M. flexor digitorum longus* in the monk parakeet. The following muscles are absent in both species: *M. plantaris*, *M. popliteus*, *M. adductor digiti II*, and *M. extensor brevis digiti III*. Finally, both species share the presence of the branch from the *M. extensor digitorum longus* to the hallux. This condition is also present in the mousebirds, and it is evidence of common ancestry among these groups (Berman and Raikow, 1982; McKittrick, 1991).

Character mapping shows that presence or absence of the *M. ambiens* (Fig. 8) is highly variable in Psittaciformes (Garrod, 1874b); for instance, it is present in *Ara*, *Cyanoliseus*, *Nestor*, *Psittacus* (Garrod, 1873, 1874b; Beddard, 1898), *Bolborhynchus*, *Poicephalus* (Garrod, 1874b; Beddard, 1898), *Aratinga*, *Pionites*, and *Psilopsiagon*

(Brereton, 1963 in Mayr, 2010). This muscle is also present in the kakapo *Strigops*, which has mainly terrestrial habits, although in this case it is inserted onto the *ligamentum patellae* instead of one of the digit flexors as seen in other psittaciforms (Garrod, 1873, 1874b; Beddard, 1898). Mayr (2010), based on phylogenetic hypotheses, states that the *M. ambiens* is lost in the Cacatuinae, in the Psittaculini + Platycercini + Cyclopsittini + Loriinae clade, in the *Coracopsis* + *Psittichas* clade and in the New World parrots *Forpus*, *Pyrhura*, *Brotogeris*, *Pionopsitta*, *Pionus*, and *Amazona*. It was assumed that the *M. ambiens* would be absent in *Myiopsitta* (Mayr, 2010), because it is absent in other members of the same subclade (*Brotogeris*, *Pionopsitta*, and *Pionus* “amazons and allies,” Tavares et al., 2006). As noted by Garrod

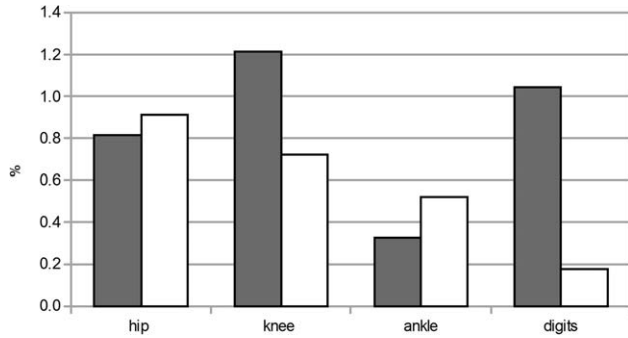


Fig. 7. *Myiopsitta monachus*, percentage of the muscles of the hindlimb with respect to the body mass grouped in flexors (grey) and extensors (white) at the different joints.

(1874b), the presence of the *M. ambiens* is plesiomorphic in neornithine birds, a condition retained by the monk parakeet (Fig. 8) that disappears in most members of the order.

The different types of connections between feet tendons have been used over a century as higher-level taxonomic characters (Raikow, 1985). The relationship between the *M. flexor digitorum longus* and the *M. flexor hallucis longus* in the monk parakeet is type I in Gadow's classification (1894). This is the same type that the author described for Psittaciformes like *Nestor* and *Ara* (Fig. 8), where the tendon of *M. flexor hallucis longus* inserts on the hallux but is connected by a *vinculum* to the tendon of *M. flexor digitorum longus*. Berman (1984) concluded that the white-fronted amazon has the type X because the flexors are connected by individual branches to each digit. In both type I and type X, the hallux is only flexed by the *M. flexor hallucis longus*, whereas the other digits are flexed by the action of both the *M. flexor hallucis longus* and the *M. flexor digitorum longus* (Berman, 1984; Raikow, 1985).

Finally, the *M. fibularis longus* is developed in terrestrial basal Psittaciformes (e.g., the kakapo *Strigops habroptilus*) but poorly developed in arboreal species which instead exhibit a large *M. fibularis brevis*. This highlights the functional importance of this muscle during arboreal locomotion (Fig. 8, see below).

Comparisons of Muscle Mass

In the arboreal monk parakeet, the mass of hindlimb muscles relative to body mass (6.5%) was similar to other zygodactyl birds like Picidae (6.04–12.98%; Hartman, 1961), and climbing birds like Dendrocolaptidae (6.57–7.65%, Hartman, 1961). Compared to the parrots, these proportions are much lower in birds that exclusively use their wings for locomotion, such as Hirundinidae (1.80–2.90%, Hartman, 1961). This proportion is higher in birds with terrestrial locomotion like Phasianidae (12.16–16.38%, Hartman, 1961). We are aware

that such comparisons between unrelated birds might be questionable, but hindlimb and body mass ratio data is indicative of the potential power of a muscle during locomotion (Hartman, 1961).

The basic adaptation for an arboreal locomotion is a strong grip (Raikow, 1985) and the independent action of the flexor muscles of each finger (Owre, 1967). This is consistent with our results, which indicate high potential force production ($PCSA_{FDL}$: 10.179 mm²; $PCSA_{FHL}$: 6.157 mm²) and a predominance of the mass of the flexor muscles of the digits (see below). Further studies on the total mass of the flexor and extensor muscles at each joint would be required for comparisons with other birds.

Functional Anatomy of Muscles and Arboreal Habits

Arboreal habits involve a variety of movements and postures including perching, climbing, hanging (restricted to a few birds), and moving easily among trees. In the case of Psittaciformes, the beak also helps during motion. These abilities, together with handling food, are associated with the zygodactyl digit arrangement and some peculiarities in the muscles responsible for flexion and rotation of the distal joints.

In the monk parakeet, the flexion force of the *M. tibialis cranialis* is relatively high compared to other Aves as a consequence of: (1) the enlargement of the attachment areas of its two heads of origin (Bock, 1974); (2) the high PCSA value (11.298 mm²) compared with other values calculated; and (3) a more distal insertion on the *tarsometatarsus*. Altogether, these traits and anatomical arrangements increase the effectiveness of the dorsal flexion from a biomechanical point of view (Volkov, 2004). The increased development of the TC is associated with the capacity of the monk parakeet to remain suspended by its hindlimbs, as has been suggested for Coliiformes, which also have TC with two heads of origin (Berman and Raikow, 1982). Moreover, the high force-generating capacity of the *M. fibularis brevis* ($PCSA_{FB}$: 8.811 mm²) is associated with a more effective flexion of the ankle joint, a feature shared with some passerines with similar upside-down hanging abilities (Moreno, 1990). The function of the *M. fibularis brevis* has been broadly discussed (e.g., Mitchell, 1913; Hudson, 1937; Owre, 1967; Raikow, 1985; Moreno, 1990). However, its role in the inward rotation of the *tarsometatarsus* (Zinoviev, 2000) and its increased development in monk parakeets seems likely to improve their food-handling skills.

The development of the *M. fibularis brevis* typically occurs in conjunction with a reduction in the *M. fibularis longus* (Mitchell, 1913), as it is seen in the monk parakeet ($PCSA_{FL}$: 3.576 mm²) and

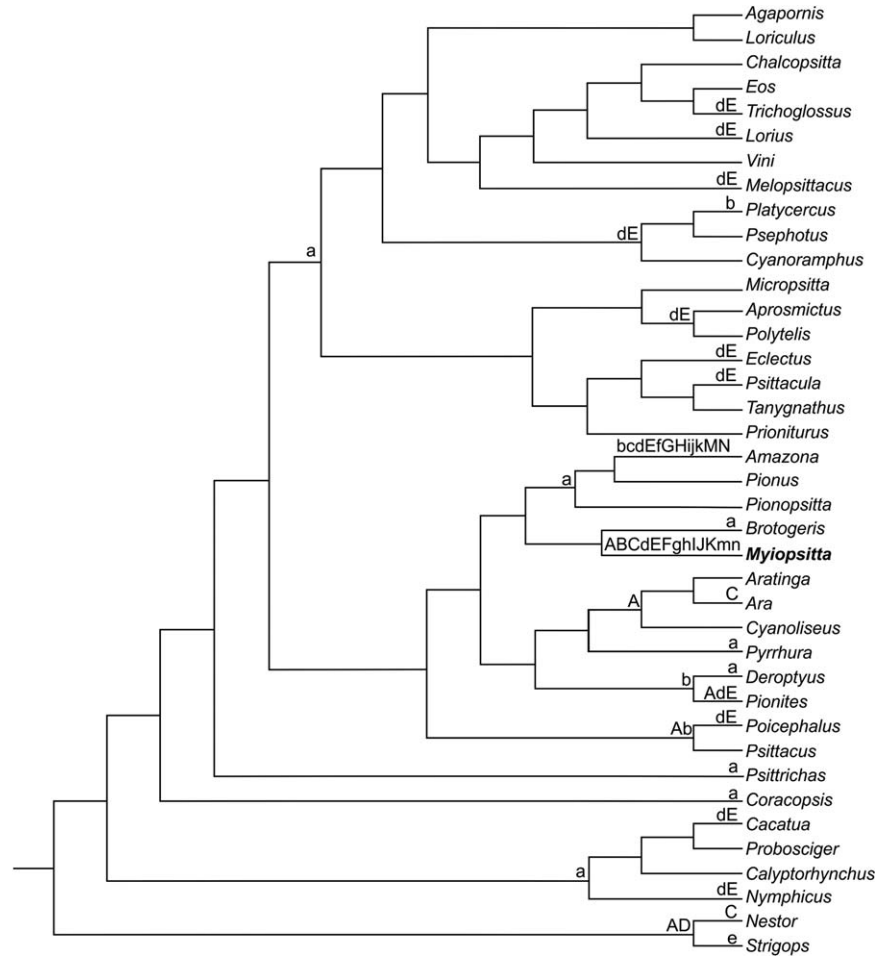


Fig. 8. Phylogenetic diagram plotting occurrence of morphologic traits in Psittaciformes. Presence (A) or absence (a) of the *M. ambiens*, tendon of insertion of *M. tibialis cranialis* single (B) or double (b), type I (C) or X (c) of connection between the *M. flexor digitorum longus* and the *M. flexor hallucis longus*, *M. fibularis longus* developed (D) or weak (d), *M. fibularis brevis* developed (E) or weak (e), *M. iliofibularis* with one belly (F) or two (f), presence (G) or absence (g) of the *M. extensor hallucis longus*, presence (H) or absence (h) of the *M. extensor digitorum brevis medialis*, *M. flexor perforans et perforatus digiti II* perforated (I) or not perforated (i) by the *M. flexor digitorum longus*, presence (J) or absence (j) of the *M. flexor perforatus digiti II* femoral origin, presence (K) or absence (k) of the *M. abductor digiti II*, presence (M) or absence (m) of the *M. extensor brevis digiti IV*, presence (N) or absence (n) of the *M. lumbricalis*.

most other arboreal Psittaciformes (Mitchell, 1913; Berman, 1984; Fig. 8). By contrast, the *M. fibularis longus* is well developed in the kakapo, a non-flying nocturnal parrot that easily moves in trees but also is fast on the ground (Mitchell, 1913; Fig. 8). This pattern of differential development in both *mm. fibularis* was also found between terrestrial and arboreal cuckoos (Berger, 1960).

Although the precise role of the flexor muscles of toes is unclear in functions like grasping and climbing (Sustaita et al., 2012), their accurate control and independent action are likely important for food manipulation and balance readjustment during arboreal locomotion (Owre, 1967; Berman, 1984; Raikow, 1985). This is evidenced in the large proportion of muscle mass involved in the flexion of the digits (Table 1, Fig. 7). Flexor muscles may act together or independently. Coordinated toe grasping is carried out by the simultaneous action

of the *M. flexor digitorum longus* and the *M. flexor hallucis longus*, which are connected by a *vinculum*. The independent action of flexor muscles in each toe while perching and moving in trees allows displacement of the center of mass of the animal during this unstable equilibrium (Owre, 1967). The *M. ambiens* assists and reinforces the action of the *M. flexor perforatus digiti II* in the monk parakeet. It has been postulated that in Psittaciformes the tendon of insertion of the *M. ambiens* contributes to the *aponeurosis communis fibularis* that gives origin to some crural muscles (Zinoviev, 2003b). However, our dissections revealed that the tendon of insertion of the *M. ambiens* crosses the knee joint, extends into the lateral region of the *tibiotarsus*, and inserts on the fleshy portion of the *M. perforatus flexor digiti II* (Fig. 3d). The simultaneous flexion and adduction of the second toe plays an important role in

arboreal locomotion, especially when the bird perches on thin branches (Zhang et al., 2012). In the monk parakeet, the absence of the *M. adductor digiti II* is functionally compensated by the action of the *M. flexor perforans digiti II* that inserts on the lateral side of digit II (Raikow, 1985), instead of inserting on the ventral surface as it usually does. The presence of accessory muscle insertion branches (e.g., the branch that *M. extensor digitorum longus* sends to the hallux) and the diversification and development of intrinsic muscles provide more delicate control of the digits (Berman and Raikow, 1982; Berman, 1984; Raikow, 1985). These features have been associated with dexterity and fine motor control in manipulating food (Sustaita et al., 2012 and bibliography cited therein). Finally, the *M. extensor propius digiti III* of the foot supplements the action of *M. extensor digitorum longus*.

ACKNOWLEDGMENTS

The authors are grateful to Federico J. Degrange and Luis Pagano for providing the specimens dissected and to CONICET for its permanent support. Authors thank Prof. Matthias Starck and two anonymous reviewers whose comments improved this manuscript. Authors appreciate the improvements in English usage made by Rebecca Cramer through the Association of Field Ornithologists' program of editorial assistance.

LITERATURE CITED

- Baumel JJ, King AS, Breazile JE, Evans HE, Vanden Berge JC. 1993. Handbook of Avian Anatomy: Nomina Anatomica Avium, 2nd ed. Cambridge, MA: Publications of the Nuttall Ornithological Club, No. 23, p 779.
- Beddard FE. 1898. The Structure and Classification of Birds, London: Longmans Green and Co.
- Beddard FE, Parsons FG. 1893. On certain points in the anatomy of parrots bearing on their classification. Proc Zool Soc London 1893:507–514.
- Berger AJ. 1956. Anatomical variation and avian anatomy. Condor 58:433–441.
- Berger AJ. 1960. Some anatomical characters of the Cuculidae and the Musophagidae. Wilson Bull 72:60–103.
- Berman SL. 1984. The hindlimb musculature of the white-fronted amazon (*Amazona albifrons*, Psittaciformes). Auk 101:74–92.
- Berman SL, Raikow RJ. 1982. The hindlimb musculature of the mousebirds (Coliiformes). Auk 99:41–57.
- Bock WJ. 1974. The avian skeletomuscular system. In: Farner DS, King JR, editors. Avian Biology 4. London: Academic Press, pp 119–257.
- Bock WJ. 1994. Concepts and methods in ecomorphology. J Biosci 19:403–413.
- Bock WJ, DeWitt Miller W. 1959. The scansorial foot of the woodpeckers, with comments on the evolution of perching and climbing feet in birds. Am Mus Novit 1931:1–45.
- Bock WJ, Shear ChR. 1972. A staining method for gross dissection of vertebrate muscles. Anat Anz 130:222–227.
- Collar NJ. 1997. Family Psittacidae (Parrots). In: del Hoyo J, Elliott A, Sargatal J, editors. Handbook of the Birds of the World, Vol. 4: Sandgrouse to cockos. Barcelona: Lynx Editions, pp 280–477.
- Gadow H. 1894. Muscular system. In: Newton A, editor. A Dictionary of Birds, Part III (moa-sheathbill). Adam and Charles Black, London, pp 602–620.
- Garrod AH. 1873. On certain muscles of the thigh of birds and their value in classification. Part I. Proc Zool Soc London 41: 626–644.
- Garrod AH. 1874a. On certain muscles of the thigh of birds and their value in classification. Part II. Proc Zool Soc London 42: 111–123.
- Garrod AH. 1874b. On some points in the anatomy of the parrots which bear on the classification of the suborder. Proc Zool Soc London 42:586–598.
- Garrod AH. 1876. Notes on the anatomy of certain parrots. Proc Zool Soc London 44:691–692.
- Giebel C. 1862. Zur Anatomie der Papageien nach Chr. Nitzsch's Untersuchungen mitgeteilt. Zeitschrift für die gesamten Naturwissenschaften. Bd. 19. Hf. 2. S.:133–152.
- Hartman F.A. 1961. Locomotor mechanisms of birds. Smithsonian Misc Collections 143:1–91.
- Hudson GE. 1937. Studies on the muscles of the pelvic appendage in birds. Am Midl Nat 18:1–108.
- Liem KF, Bemis WE, Walker WF, Grande L. 2001. Functional Anatomy of the Vertebrates, Orlando: Harcourt College Publisher, p 766.
- Mayr G. 2010. Parrot interrelationships – morphology and the new molecular phylogenies. Emu 110:348–357.
- McKittrick MC. 1991. Phylogenetic analysis of avian hindlimb musculature. Misc Publ Mus Zool Univ Mich 179:1–85.
- Mitchell PC. 1913. The peroneal muscles in birds. Proc Zool Soc London 83:1039–1072.
- Moreno E. 1990. Form and function of the fibularis brevis muscle in some passerine birds. Ann Zool Fenn 27:3–9.
- Mosto MC, Carril J, Picasso M.B.J. 2013. The hindlimb myology of milvago chimango (Polyborinae, Falconidae). J Morphol 274:1191–1201.
- Owre OT. 1967. Adaptations for locomotion and feeding in the Anhinga and the Double-crested Cormorant. Ornithol Monogr 6:1–138.
- Pennycuik CJ. 1996. Stress and strain in the flight muscles as constraints on the evolution of flying animals. J Biomech 29: 577–581.
- Picasso M.B.J, Tambussi CP, Mosto MC, Degrange FJ. 2012. Crecimiento de la masa muscular del miembro posterior del ñandú grande (*Rhea americana*) durante la vida postnatal. Rev Bras Ornitol 20:1–7.
- Raikow RJ. 1985. Locomotor System. In: King AS, Mc Lelland J, editors. Form and Function in Birds, Vol. 3. London: Academic Press, pp 57–147.
- Raikow RJ. 1987. Hindlimb myology and evolution of Old World suboscine passerine birds (Acanthisittidae, Pittidae, Philepittidae, Eurylaimidae). Ornithol Monogr 41:1–81.
- Raikow RJ. 1994. A phylogeny of the woodcreepers (Dendrocopidae). Auk 111:104–114.
- Smith NC, Wilson AM, Jaspers KJ, Payne RC. 2006. Muscle architecture and functional anatomy of the pelvic limb of the ostrich (*Struthio camelus*). J Anat 209:765–779.
- Sustaita D. 2008. Musculoskeletal underpinnings to differences in killing behavior between North American Accipiters (Falconiformes: Accipitridae) and Falcons (Falconidae). J Morphol 269:283–301.
- Sustaita D, Pouydebat E, Manzano A, Abdala V, Hertel F, Herrel A. 2012. Getting a grip on tetrapod grasping: form, function, and evolution. Biol Rev 88:380–405.
- Tavares ES, Baker AJ, Pereira SL, Yumi Miyaki C. 2006. Phylogenetic relationships and historical biogeography of neotropical parrots (Psittaciformes: Psittacidae: Arini) inferred from mitochondrial and nuclear DNA sequences. Syst Biol 55:454–470.
- Vanden Berge JC. 1970. A comparative study of the appendicular musculature of the Order Ciconiiformes. Am Midl Nat 84: 289–364.

- Volkov SV. 2004. The hindlimb musculature of the true owls (Strigidae: Strigiformes): Morphological peculiarities and general adaptations. *Ornithologia* 31:154–174.
- Wright TF, Schirtzinger EE, Matsumoto T, Eberhard JR, Graves GR, Sanchez JJ, Capelli S, Müller H, Scharpegge J, Chambers GK, Fleischer RC. 2008. A multilocus molecular phylogeny of the parrots (Psittaciformes): Support for a Gondwanan origin during the Cretaceous. *Mol Biol Evol* 25:2141–2156.
- Zinoviev AV. 2000. Function of *M. fibularis brevis* in birds and mechanism of stabilizing intertarsal joint. *Zool Zh* 79:1337–1343 (in Russian, English abstract).
- Zinoviev AV. 2003a. About terminology of short extensor muscles of the avian foretoes. *Ornithologia* 30:127–131 (in Russian, English abstract).
- Zinoviev AV. 2003b. Common aponeurosis of origin of avian crural muscles as a key object of the avian hindlimb myology. *Ornithologia* 30:132–135 (in Russian, English abstract).
- Zinoviev AV. 2007. A modern view on the functional content of the GarrodÇs muscular formula. *Zool Zh* 86:978–988. (in Russian, English abstract).
- Zinoviev AV. 2010. Comparative anatomy, structural modifications and adaptive evolution of avian apparatus of bipedal locomotion, Moscow: KMK Scientific Press Ltd, p 285. (in Russian).
- Zhang Z, Vanden Berge JC, Sun YH. 2012. Descriptive anatomy of the pelvic appendage myology of the endemic Chinese grouse (*Tetrastes sewerzowi*). *Wilson J Ornithol* 124:328–337.